ELSEVIER

PII: S0032-3861(97)10119-7

Polymer Vol. 39 No. 15, pp. 3365–3372, 1998

0032-3861/98/$19.00+0.00

Physical characterization of a polyolefinic thermoplastic elastomer

Ying Yang, Tsuneo Chiba, Hiromu Saito and Takashi Inoue*
Department of Organic and Polymeric Materials, Tokyo Institute of Technology, Ookayama, Megoru-ku, Tokyo 152, Japan
(Received 23 June 1997; revised 25 August 1997; accepted 16 September 1997)

Physical characterization of a commercial polyolefinic thermoplastic elastomer (TPE), Santoprene®, was undertaken to understand the elastomeric nature of the two-phase material in which rubber particles are dispersed in a matrix of polypropylene (PP). Dynamic mechanical analysis showed that the PP matrix contains a small amount of rubber. PP crystal lamellae in rubber particles in a well-annealed sample were observed by transmission electron microscopy, suggesting that PP had been occluded in the rubber phase. Such partial phase-mixing may be caused by homogenization under high shear during dynamic vulcanization. Wide angle X-ray diffraction (WAXD) studies showed that PP crystallites in TPE are smaller than those in neat PP. That is, the occluded rubber in the PP matrix may play the role of impurity to render the smaller crystallites. By WAXD analysis on crystal orientation and its relaxation in stretching and releasing processes, it was shown that the smaller crystallites suffer less plastic deformation and, rather, play the role of tie points to provide the elastic properties of the PP matrix itself. About 40 wt% of process oil was found to be loaded on TPE; however, the oil seems to play a minor role in providing the elastomeric character.

(Keywords: polypropylene; thermoplastic elastomer; strain recovery)

INTRODUCTION

Polyolefinic thermoplastic elastomer (TPE) is prepared by the dynamic vulcanization of the blend of polypropylene (PP) with ethylene–propylenediene rubber (EPDM); e.g. by melt-mixing a 40/60 PP/EPDM blend in the presence of curatives, such as sulfur, accelerators and peroxides[1,2]. The dynamic vulcanization yields two-phase material in which cured EPDM particles having a diameter of a few micrometers are dispersed in the PP matrix. The two-phase material thus prepared can be fabricated into end-use parts by the conventional melt processing for thermoplastics. This melt processability is natural because the matrix consists of thermoplastic polymer (PP). However, the question is why the melt-processed TPE behaves like a vulcanized rubber at ambient temperature. That is, why is the TPE able to shrink back from the highly deformed states, even though the matrix consists of the ductile polymer? In other words, why is the bulk property of TPE not governed by the ductile character of the matrix but mostly by that of the dispersed phase?

To answer this question, we carried out elastic–plastic analysis on the deformation mechanism of the two-phase system by the finite element method (FEM)[3]. FEM analysis revealed that, even at the highly deformed states at which almost the whole matrix has been yielded by the stress concentration, the ligament matrix between rubber inclusions in the stretching direction is locally preserved within an elastic limit and it acts as an in situ formed adhesive for interconnecting the rubber particles, providing a key mechanism of the strain recovery in the two-phase system. In the FEM analysis, the matrix was implicitly assumed to consist of neat PP. However, one has to be suspicious about it; i.e. the matrix might be a mixture of PP and EPDM. The background is as follows.

Most pairs of dissimilar polymers are immiscible, but several pairs follow the phase diagram; i.e. the polymers are miscible at low temperatures but immiscible at higher temperatures. Such phase behaviour is called lower critical solution temperature (LCST)-type behaviour. The phase behaviour is in a quiescent state. It is becoming obvious that the phase behaviour is affected by shear fields. At high shear rates, phase mixing is induced by shear flow and the LCST elevates[4–6]. The shear effect was taken into account to understand the structure development in polymer blends during melt processing, such as extrusion[7] and injection moulding[8].

In the dynamic vulcanization, two polymers are subjected to high shear rates and a crosslink reaction is imposed on one of the polymers so that the phase mixing induced by shear flow might be somewhat preserved in the processed TPE by the crosslinking. Then, in the case of PP–EPDM TPE for instance, the TPE matrix could be a mixture of PP with EPDM and the presence of EPDM would change the structure and properties of the matrix to be favourable to the elastomeric character of TPE. In this paper, we selected one of the commercial polyolefinic TPEs and investigated its structure and properties from such a standpoint.

EXPERIMENTAL

The PP-based TPE used in this study was a commercial product supplied by Mitsubishi Monsanto Co., Santoprene® #201-73. The TPE is believed to be prepared by dynamic vulcanization of isotactic polypropylene (iPP)/EPDM blend. An iPP supplied by Mitsui Toatsu Chemicals Inc., J3HG, was used as a neat PP. High density polyethylene

* To whom correspondence should be addressed

(HDPE) supplied by Showadenko, 5050, was used to prepare a control blend with PP, because in the case of a wide composition distribution of EPDM, the EPDM might contain neat PE.

The processing oil in the original TPE was extracted by xylene at room temperature. After the extraction, the TPE was dried in vacuum at 50°C for 48 h. The original TPE before the extraction was coded as OTPE, and the oil-extracted TPE as ETPE.

Both OTPE and ETPE were compression-moulded into films at 220°C then quenched in water. Some of the quenched films were heated to 210°C for 5 min, then quenched to 130°C and crystallized isothermally at that temperature for 15 h.

IPP was melt mixed with HDPE in a miniature moulder mixer (Mini-Max, Model CS-183MMX, Custom Scientific Instruments, Inc.) at 210°C, then quenched in water. The iPP/HDPE blend was used as a control sample for wide angle X-ray diffraction (WAXD) studies.

Dynamic mechanical behaviour was measured using a Toyoseiki Dynamic Mechanical Analyzer at 100 kHz at a heating rate of 2°C min^{-1}. The temperature dependence of the dynamic loss (tan δ) was obtained.

The differential scanning calorimeter (d.s.c.) measurements were carried out using a Seiko SII DSC 6200. The specimens were heated and cooled at a rate of 20°C min^{-1} in an N_2 atmosphere. The melting temperature and the enthalpy of fusion were obtained from the maximum and the area of the endothermic peak respectively. The crystallinity X_C was calculated by the enthalpy of fusion per gram of iPP (or that per gram of blend) and the heat of fusion of iPP crystal (209 J g^{-1})[9].

The tensile stress–strain curves at room temperature were obtained using a tensile testing machine (Tensilon UTM-II-20, Toyo Baldwin Co., Ltd) with crosshead rate of 10 mm min^{-1}. After the pre-setting strain was reached, the strain was released at the same rate as the stretching one. After the strain reached zero, the sample was released from the clamps and the residual strain was measured at certain time intervals.

For transmission electron microscopy (TEM), the ultrathin sections, about 70 nm thick, were obtained using an ultra cryomicrotome, Ultracut N, Reichert–Nissei, at −80°C. The sections were stained by RuO_4 vapour for 10 min at 50°C. The morphology of the TPE was examined by a JEM 100 CX transmission electron microscope, Jeol Co., at 100 kV acceleration voltage.

The infrared spectra were obtained using a Jasco FTIR-410 infrared spectroscope.

The WAXD pattern was observed by a Rigaku Denki RU-200 X-ray diffraction apparatus using an R-AXIS II D image plate. The radiation from the Cu anode was reflected from a graphite monochromator to obtain monochromatic Cu Kα radiation with a wavelength of 0.1541 nm. The generator was operated at 40 kV and 100 mA. For in situ tensile tests in WAXD, a mini-tensile machine was used.

RESULTS AND DISCUSSION

The TEM micrograph of the original TPE (OPTE) is shown in *Figure 1*. One can see that the OTPE has a two-phase morphology. The dark regions can be assigned to the rubber phase (EPDM) since RuO_4 preferentially stains the amorphous phase[10,11]. The rubber particles are not uniform in size. The average diameter is 3 μm.

Referring to the literature[2,12], TPE contains a lot of mineral oil. *Figure 2* is the curve of the weight loss *versus* the extraction time. After about 240 h extraction, the weight loss levels off. This result suggests that the TPE contains approximately 40% of process oil.

The temperature dependence of the dynamic loss (tan δ) is shown in *Figure 3*. Two tan δ peaks appear in both OTPE and ETPE specimens. They could be assigned to the T_g of iPP and that of rubber phase. Both the T_g values of the rubber and iPP phases in the TPE shift to high temperatures and the tan δ values reduce with oil extraction. The reduction of tan δ in the rubber phase with oil extraction is greater than that in the iPP phase, suggesting that, at ambient temperature, the oil preferentially stays in the rubber phase.

One can see that the T_g of the iPP phase in ETPE is lower than that of neat iPP. A T_g shift in ETPE should be caused by the mixing with the rubber because the oil had been extracted, as shown in *Figure 2*. The T_g of the iPP phase in OTPE is also lower than that of neat iPP. This may be attributed to the mixing with both oil and rubber.

D.s.c. thermograms provide supplemental information about the partial phase-mixing in the TPE. *Figure 4* and *Figure 5* are the d.s.c. thermograms of the TPE during

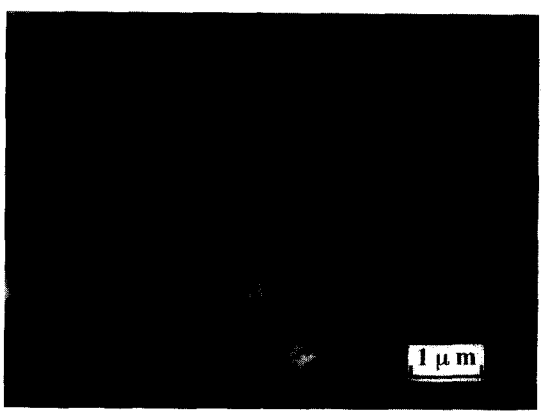

Figure 1 TEM micrograph of the original TPE

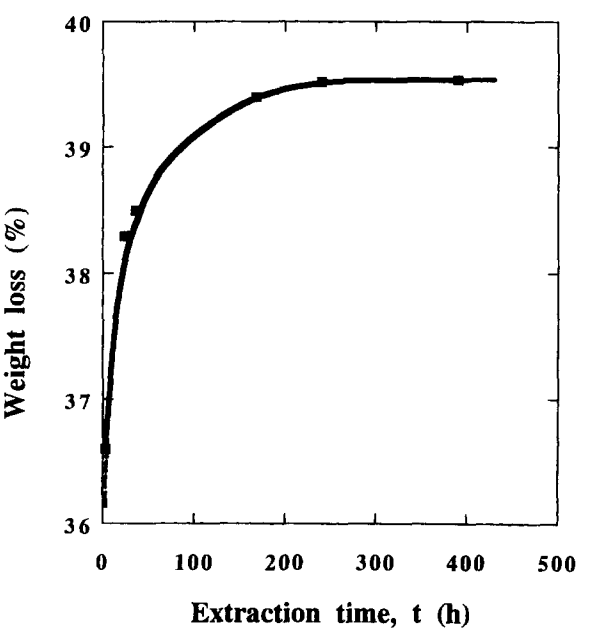

Figure 2 Weight loss by extraction with xylene at room temperature (25°C)

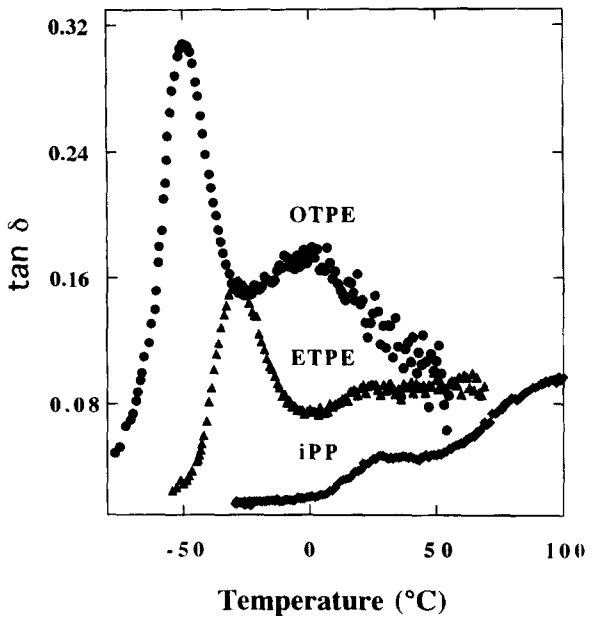

Figure 3 Dynamic loss *versus* temperature curves for neat PP, OTPE and ETPE. All specimens were melt-pressed at 210°C and quenched in water

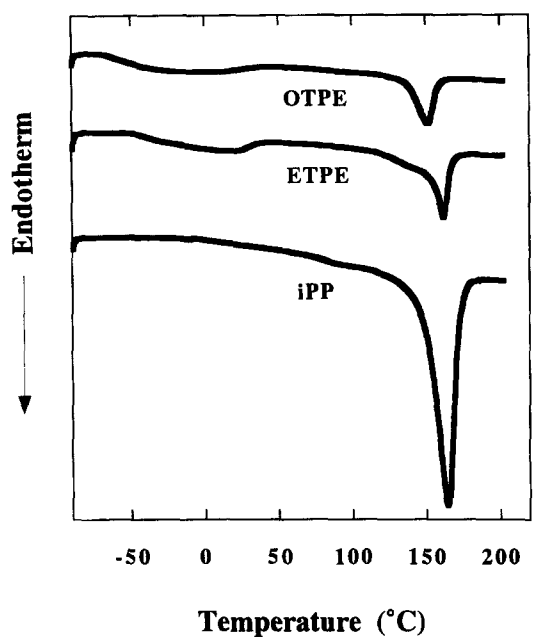

Figure 4 D.s.c. thermograms for neat PP and the TPEs in heating mode

heating and cooling scans respectively. The thermal characterization data are summarized in *Table 1*. In the heating scan, even for OTPE, one can see that one melting peak appears at 151°C. This corresponds to the melting point of iPP crystallites. The ETPE has a slightly lower melting point than that of neat iPP. This T_m depression may be attributed to several reasons, such as mixing with the rubber or smaller size and disordering of the iPP crystallite. We shall discuss this later.

Figure 5 shows that the crystallization temperature T_c of iPP in ETPE is higher than that in neat iPP, whereas the T_c of iPP in OTPE is lower than that of neat iPP. The elevation of the T_c in the ETPE may be ascribed to the lower T_g effect caused by the phase mixing with rubber.

The results in *Figures 3–5* imply that in the TPE the matrix is not neat iPP, but is an iPP-rich phase containing a small amount of rubber. Such phase-mixing could be

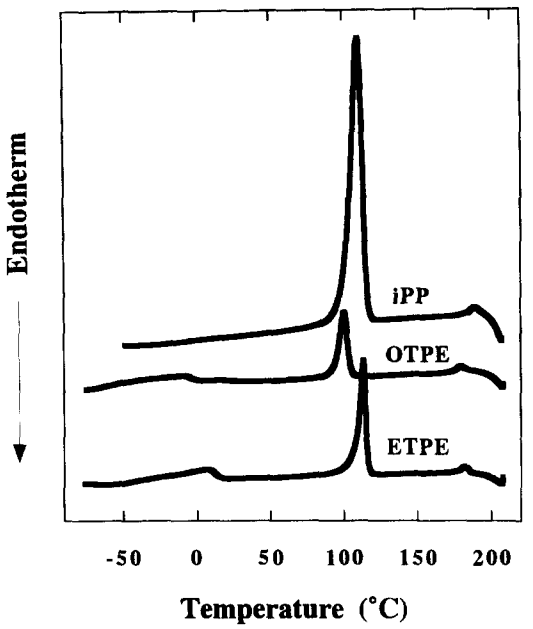

Figure 5 D.s.c thermograms for neat PP and the TPEs in cooling mode

achieved under high shear[13,4–8] during melt-mixing in the rubber phase; i.e. it may not be neat rubber phase, but it contains a small amount of iPP chains which should be arrested by the crosslinking. The existence of trapped PP could be justified by watching the iPP crystals in the rubber phase using TEM.

As shown in *Figure 1*, we see no crystal structure in the rubber particles in quenched OTPE. A similar TEM image was observed for quenched ETPE. However, after isothermal annealing for a long time (15 h at 130°C), one can see iPP crystal lamellae in both OTPE and ETPE, as shown in *Figure 6*. It is interesting to note that some of the lamellae cross the interface between the iPP and rubber phases, and some of the lamellae extend deep into the rubber particles, as indicated by the arrows. This morphology provides strong evidence that the iPP had partially mixed with the rubber phase and had existed in the rubber particles before annealing. However, one has to confirm that the lamellae are not of the PE crystal but of the iPP crystal, because in the case of a wide composition distribution of EPDM the long ethylene sequences and free PE chains can crystallize. Judgement could be given by the results of d.s.c., i.r. and WAXD measurements, as follows.

Figure 7 shows the d.s.c. thermograms for neat PE, blend of HDPE/iPP (5/95) (by weight) and the annealed OTPE. It is seen that even when 5% of HDPE is mixed with iPP, the quenched blend shows an HDPE crystallite melting peak at 130°C. However, there is no such melting peak in the d.s.c. thermogram of the annealed OTPE specimen. *Figure 8* is the i.r. spectra for neat HDPE, blend of HDPE/iPP (5/95) and annealed OTPE. In the i.r. spectrum the doublet at about

Table 1 The thermal characterization by d.s.c.

Code	T_g rubber (°C)	T_m (°C)	T_C (°C)	ΔH (J g^{-1})	X_C
iPP		164.7	107	91.9	0.44
OTPE	−68.1	151.0	99.6	16.3	0.078
ETPE	−46.4	162.3	110	26.5	0.127

T_g, T_m, ΔH and X_C are from *Figure 4*. T_C is from *Figure 5*. ΔH and X_C are per weight of blend specimen

(a)

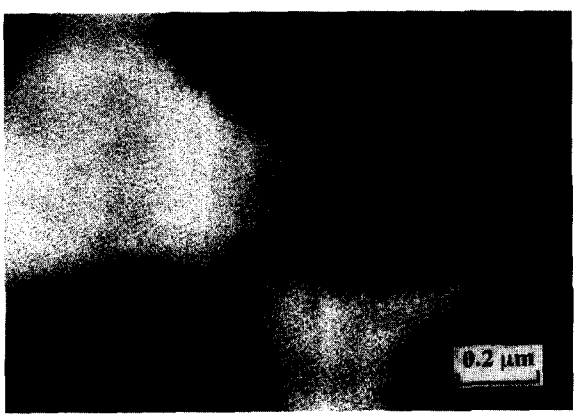

(b)

Figure 6 TEM micrographs of TPE annealed at 130°C for 15 h to attain higher crystallinity: (a) OTPE; (b) ETPE

the 720 cm^{-1} band is assigned to PE crystallites[14]. The doublet is not seen for the OTPE specimen. WAXD patterns for neat HDPE and annealed OTPE are shown in *Figure 9*. The diffraction peak characteristic of HDPE at $2\theta = 23.6°$ is not seen for the annealed OTPE. These results support the assertion that there are no PE crystallites in the annealed OTPE specimen. Then one may reach the conclusion that the lamellae in the TPE observed by TEM are not of PE but of iPP.

Then the problem is how the iPP chains can partially mix with the rubber phase. It is reported that ethylene–propylene copolymer (EPM) and EPDM are immiscible with iPP in the melt[15]. In addition, the rubber phase of the present TPE is crosslinked. The dynamic vulcanization would make the rubber less miscible with iPP. However, the immiscibility is

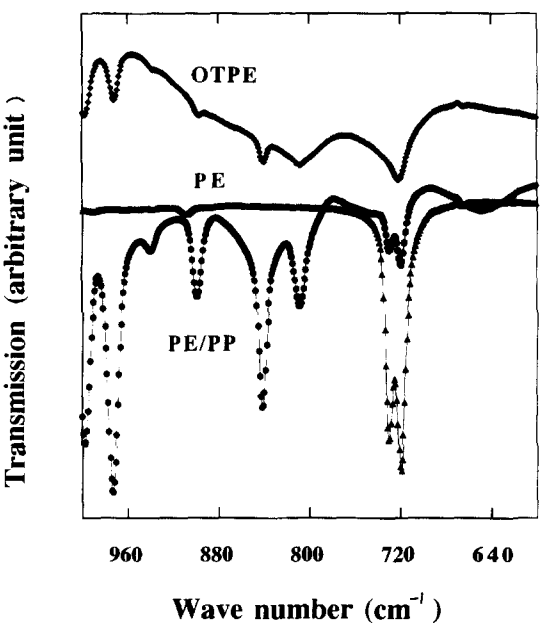

Figure 8 I.r. spectra for PE, 5/95 PE/PP blend and OTPE (same specimens as in *Figure 7*)

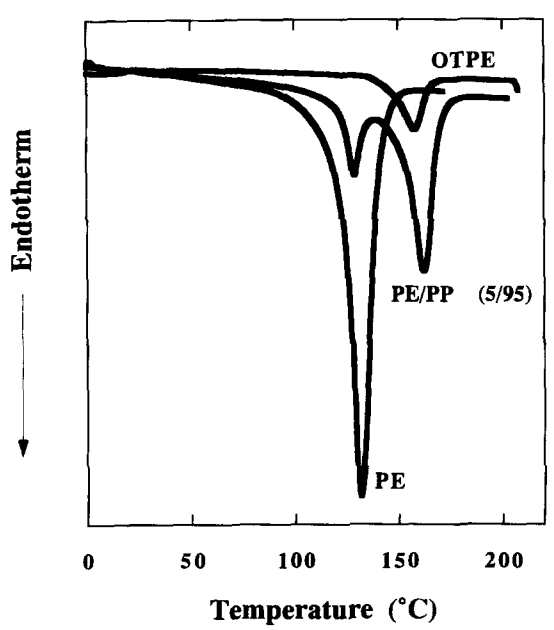

Figure 7 D.s.c thermograms for neat PE, 5/95 PE/PP blend and OTPE (after annealing at 130°C for 15 h and quenched in water)

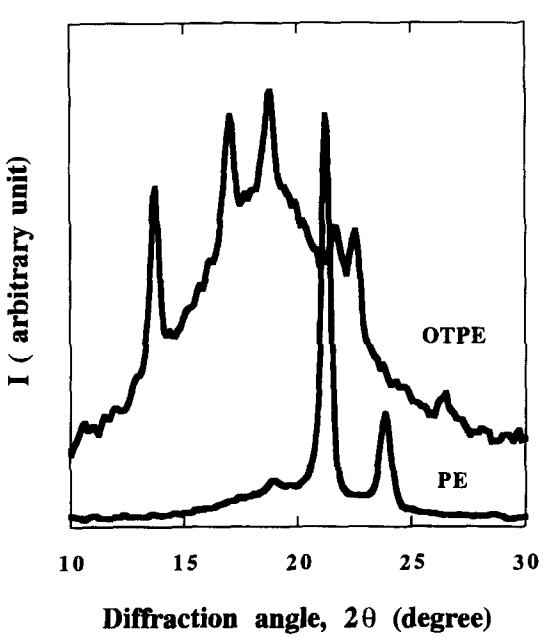

Figure 9 WAXD curves for neat PE and OTPE annealed at 130°C for 15 h

in a quiescent state. The situation might be different under high shear during melt processing, such as injection or extrusion. Studies[13,4–8] have reported that phase mixing may take place for immiscible polymer pairs under high shear. Such miscibility could be expected during melt mixing of EPR (or EPDM) with iPP. Then, this state could be arrested by the crosslinking of the rubber phase.

One should discuss further the location of iPP lamellae in *Figure 6*. The lamellae are mostly located near the interface. The iPP chains occluded in the rubber phase are immiscible with rubber in the quiescent state so that they will try to segregate. However, since they are trapped in the crosslinked rubber phase, the migration could not be completed to render just a higher concentration of iPP chains near the interface; hence this leads to iPP crystal lamellae mostly near the interface.

On the other hand, the existence of rubber in the iPP matrix could have a big influence as a polymer impurity on the crystallization of iPP to yield a crystalline morphology different from that of neat iPP. Such a morphology might render the nice strain recovery in the TPE. Next to be discussed is the crystalline morphology of iPP matrix.

The crystalline size in the perpendicular direction to the [110] plane ($2\theta = 14.16°$) was calculated from WAXD profiles using the Scherrer equation[16]. The calculated crystalline size in OTPE was 8.5 nm and was smaller than that in neat iPP (10.5 nm). The physical meaning of the crystalline size by the Scherrer equation is not fully understood and one cannot discuss quantitatively the size of crystallites. However, a smaller size by the Scherrer equation may imply more disordered crystallites. In the extreme case, the crystallites could be fragmented lamellae. In fact, there are no visible lamellae in the TEM micrograph for quenched OTPE, as shown in *Figure 1*. The fragmented lamellae could act as tie points to provide high strain recovery of the TPE.

The difference in crystalline ordering could affect the orientation behaviour of crystallites with bulk deformation. Before getting into the details of crystal orientation behaviour, it is appropriate to have a look at the bulk deformation behaviour of TPE compared with neat iPP. *Figure 10* shows the typical stress–strain curves for neat iPP, OTPE and ETPE (all quenched samples). A large residual strain is seen for neat iPP, whereas there is nice strain recovery for both OTPE and ETPE. The residual strain decreases with time after releasing the sample from the clamps. The time variation of the residual strain is shown in *Figure 11*. The residual strain levels off after *ca.* 1 h of resting. The levelled-off residual strain is shown as a function of applied strain in *Figure 12*. One sees a big difference in strain recovery behaviour between neat iPP and TPEs. There is a very small difference in strain recovery behaviour between OTPE and ETPE. This may imply that the oil does not play a major role in the strain recovery of TPE.

The WAXD results for neat iPP are shown in *Figure 13*.

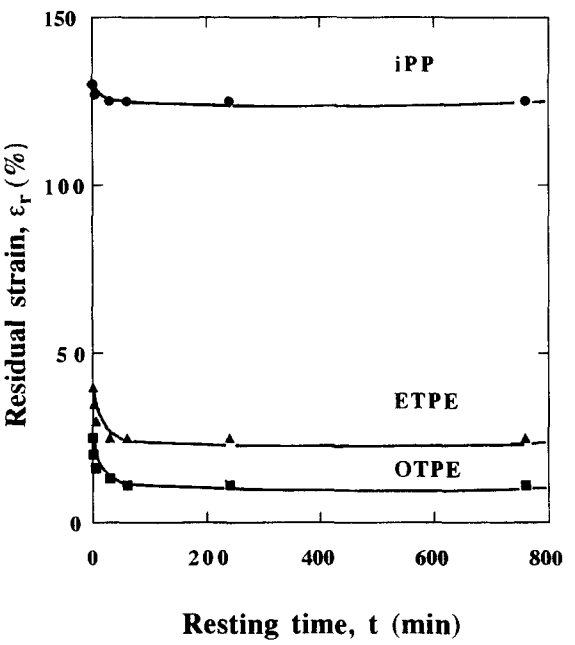

Figure 11 The residual strain after release as a function of resting time

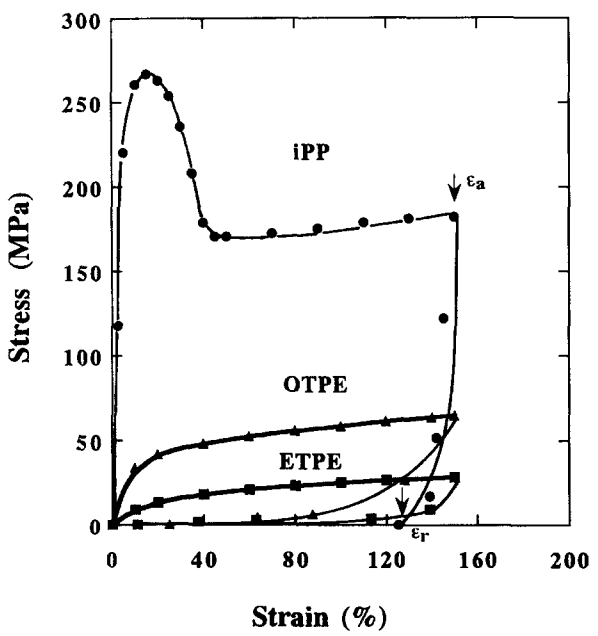

Figure 10 Typical stress–strain curves for neat PP and the TPEs; quenched in water

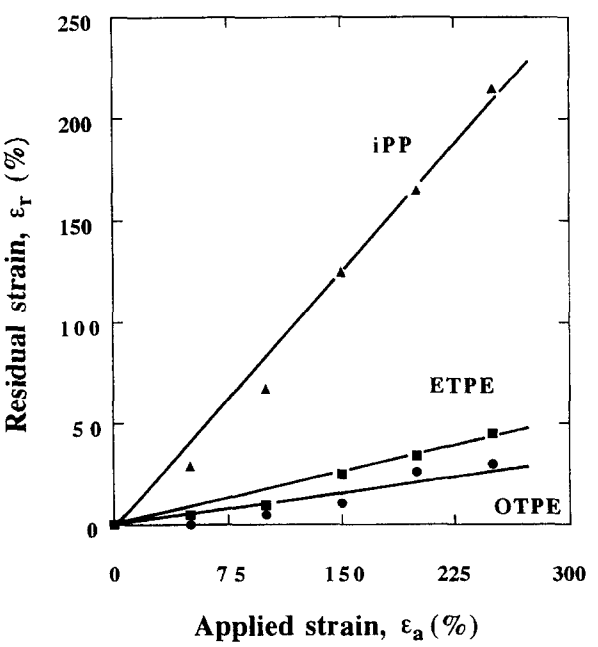

Figure 12 The residual strain (after resting 3 h) *versus* applied strain

Even at 50% elongation, the crystallites in neat iPP intensively orient in the stretching direction, as shown by the appearance of two bright arcs in the equator (*Figure 13b*) and the orientation never recovers after releasing the sample from the clamps (*Figure 13b'*). At high elongations, four arcs appear in the diagonal direction and the arcs become shorter and brighter with bulk deformation (*Figure 13c–e*). Such arcs remains unchanged upon release (*Figure 13c'–e'*), suggesting a plastic deformation of crystallites. This is the typical orientation behaviour of crystalline polymers.

Figure 14 shows WAXD patterns of OTPE. One can see that the orientation of iPP in OTPE is negligible; compare *Figure 14a* (undeformed) and *Figure 14b* (50% elongation). This is so even at 100% elongation (*Figure 14c*) and the pattern recovers almost completely to the original one after releasing the sample from the clamps (*Figure 14c* → *c'*). At 200% elongation, short arcs appear in the equator (*Figure 14e*) but the arcs disappear after release (*Figure 14e'*). Compared with the results for neat iPP in *Figure 13*, one sees that iPP crystallites in OTPE hardly orient with bulk deformation and show better recovery after releasing the bulk strain.

The plastic deformation of crystallites in neat iPP can be shown by the change in WAXD profiles with bulk deformation. *Figure 15* shows WAXD profiles of neat iPP in the equatorial direction at various strain levels. It is seen that the intensity of the [110] plane (at $2\theta = 14.16°$) increases with increasing strain (*Figure 15a*). At the high strain level (200%) the [111] plane diffraction peak (at $2\theta = 21.2°$) disappears. This may suggest a slippage in crystal lamellae. Upon release, the [113] diffraction never recovers, as shown in *Figure 15b*. Such plastic deformation of iPP crystallites is not seen for OTPE, as shown in *Figure 16*.

The crystal orientation and its recovery can be discussed more quantitatively in terms of the crystal orientation function *f*. The value of *f* was estimated by Wilchinsky's method[17] using [110] ($2\theta = 17.08°$) and [040] ($2\theta = 14.16°$) diffractions, because in the case of monoclinic iPP there is no set of diffracting [001] planes which reveals orientation of the *c*-axis directly; then, the diffraction from two sets of planes containing the *c*-axis, such as [110] and [040] could

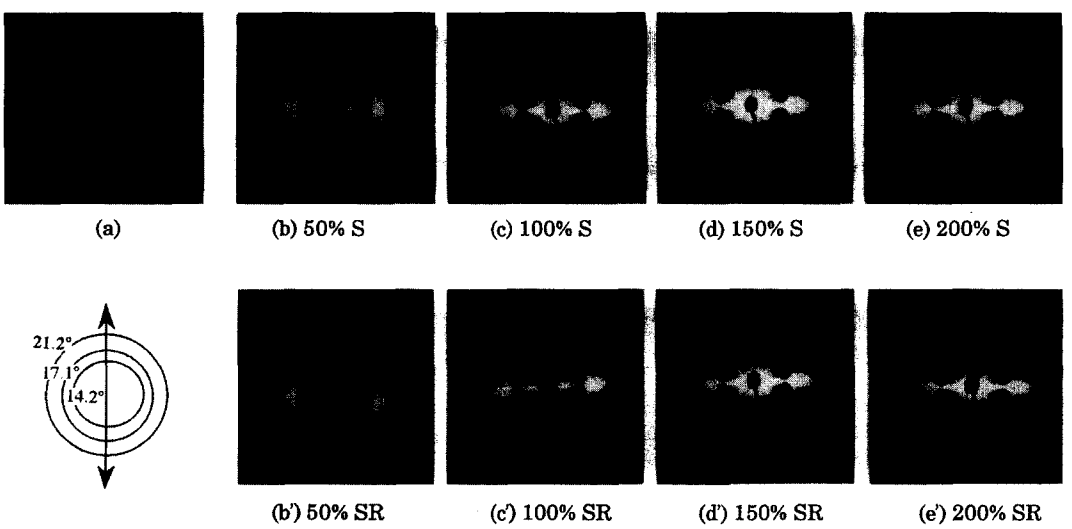

Figure 13 WAXD pattern of neat PP: (*a*) undeformed, (*b–e*) stretched (S) state and (*b'–e'*) stretched-and-released (SR) state. Number indicates percentage elongation. The stretching direction is vertical (see arrow)

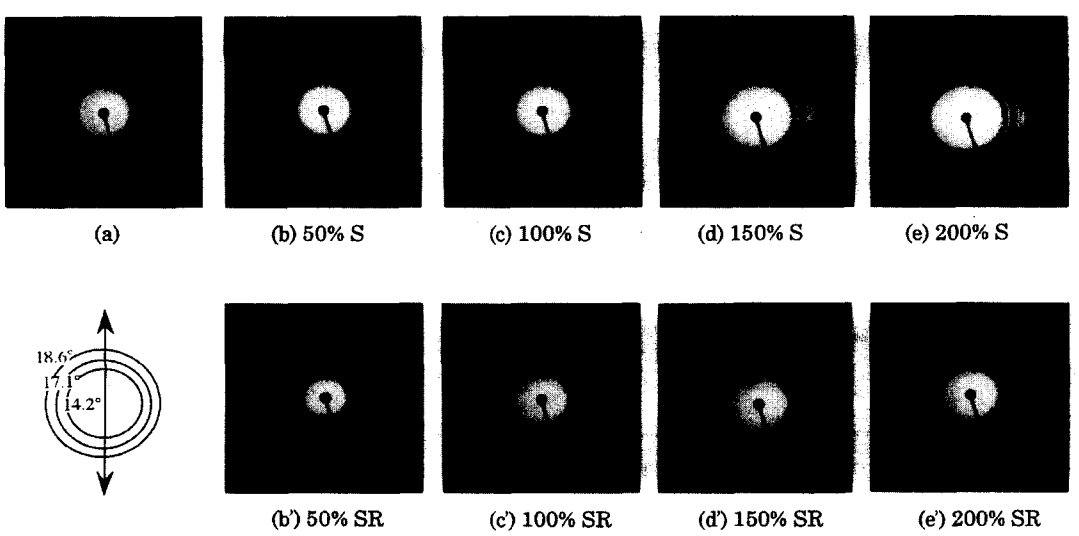

Figure 14 WAXD pattern of OTPE: (*a*) undeformed, (*b–e*) stretched (S) state and (*b'–e'*) stretched-and-released (SR) state. Number indicates percentage elongation. The stretching direction is vertical (see arrow)

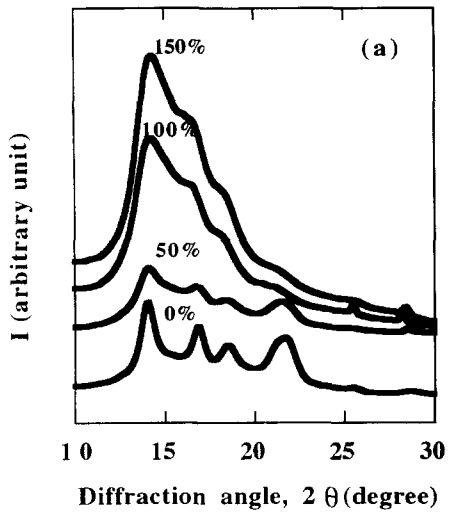

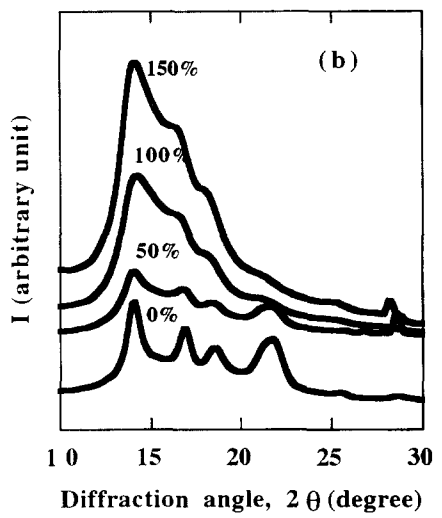

Figure 15 WAXD profile in equatorial direction for neat PP: (*a*) stretched state and (*b*) stretched to percentage elongation indicated and then released

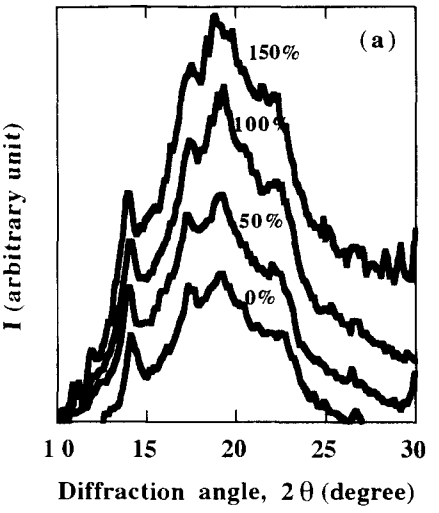

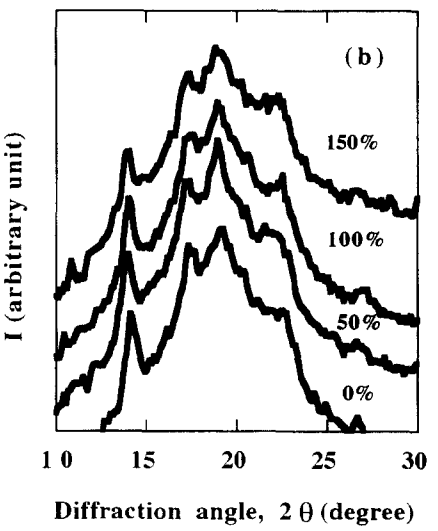

Figure 16 WAXD profile in equatorial direction for OTPE: (*a*) stretched state and (*b*) stretched to percentage elongation indicated and then released

be used to calculate the average orientation of the *c*-axis. The estimated orientation function is shown as a function of applied strain both in the as-stretched state (symbol S) and in the stretched-and-released state (SR) in *Figure 17*. The value of f for iPP is nearly double that of OTPE. After releasing the strain, the f value in iPP does not change, whereas that of OTPE decreases to lower levels. The results again suggest that the iPP crystallites in OTPE hardly orient with bulk deformation and the orientation relaxes better upon release.

The crystal orientation and relaxation behaviour of OTPE are compared with those of ETPE in *Figure 18*. Again, the oil has no significant effect on the orientation of crystallites. However, the oil seems to provide a better orientation relaxation in the recovery process in TPE.

It is interesting to note that the orientation function in the TPE does not reduce to zero upon release. This implies that, even when a certain degree of the orientation remains in the iPP crystallite, the material can shrink back to show excellent bulk strain recovery. The rotational relaxation of the orientated crystallites after release may not be the prerequisite for the strain recovery. That is, even in the oriented state, the crystallites may play the role of tie points for amorphous chains to render the elastic recovery of TPE.

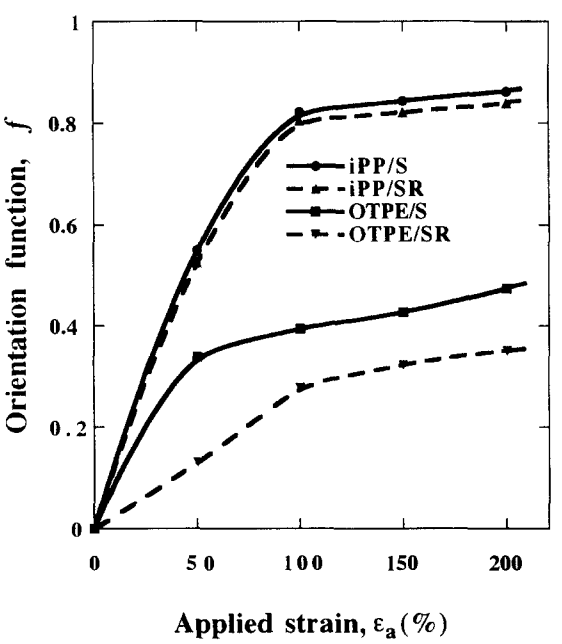

Figure 17 Orientation function *versus* applied strain for neat PP and OTPE. S: stretched state; SR: stretched-and-released

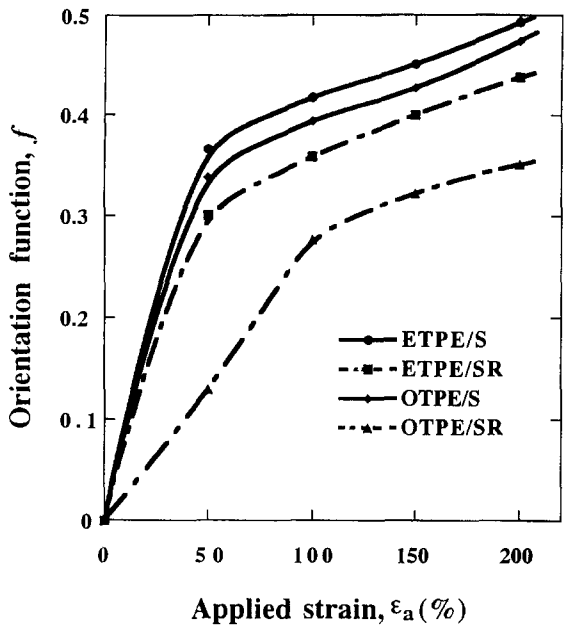

Figure 18 Orientation function *versus* applied strain for ETPE and OTPE. S: stretched state; SR: stretched-and-released

CONCLUSION

The nice strain recovery of the polyolefinic TPE may originate partly from the characteristic morphology of PP crystallites; i.e. rather fragmented crystallites caused by the presence of polymer impurity (rubber) occluded in the PP matrix under high shear during dynamic vulcanization. That is, the PP matrix itself is expected to be less ductile and more elastomeric than neat PP. The less plastic matrix may provide a favourable contribution to the key mechanism of strain recovery set up in the two-phase material composed of plastic matrix and rubber particles, as we discussed using the elastic–plastic analysis by FEM[3,8]. The large amount of oil added for TPE seems to play a minor contribution to the strain recovery of TPE. Its main function is as a processing aid.

REFERENCES

1. Coran, A. Y., in *Handbook of Elastomers—New Developments and Technology*, ed. A. K. Bhomwick and H. L. Stephens. Marcel Dekker, New York, 1988.
2. Coran, A. Y. and Patel, P., *Rubber Chem. Technol.*, 1980, **53**, 141.
3. Kikuchi, Y., Fukui, T., Okada, T. and Inoue, T., *Polym.*, 1991, **31**, 1029.
4. Katsaros, J. D., Malone, M. F. and Winter, H. H., *Polym. Eng. Sci.*, 1989, **29**, 1434.
5. Rectpr, L. P., Mazich, K. A. and Carr, S. H., *J. Macromol. Sci. Phys. B*, 1988, **27**, 421.
6. Cheikh Larbe, F. B., Malone, M. F., Winter, H. H., Halary, J. L., Leviet, M. H. and Monnerie, L., *Macromolecules*, 1988, **21**, 3532.
7. Okamoto, M. and Inoue, T., *Polymer*, 1994, **35**, 257.
8. Okamoto, M., Shiomi, K. and Inoue, T., *Polymer*, 1995, **36**, 87.
9. Brandup, S. and Immergut, E. M., *Polymer Handbook*, Vol. 5. Interscience, New York, 1975.
10. Sano, H., Usami, H. and Nakagawa, H., *Polymer*, 1987, **27**, 1497.
11. Tervoort-Engelen, Y. and Gisbergen, J. V., *Polym. Commun.*, 1991, **32**, 261.
12. Nakajima, N. and Harrell, E. R., *Rubber. Chem. Technol.*, 1983, **56**, 784.
13. Hidawi, I. A., Higgins, J. S. and Weiss, R. A., *Polymer*, 1992, **33**, 2522.
14. Tosi, C. and Ciampelli, F., *Advance in Polymer Science*, Vol. 12. Springer, Berlin, 1973.
15. Wenig, W. and Wasiak, A., *Colloid Polym. Sci.*, 1993, **271**, 824.
16. Alexander, L. E., *X-Ray Diffraction Method in Polymer Science*. Wiley-Interscience, New York, 1969.
17. Wilchinsky, Z. W., *J. Appl. Phys.*, 1969, **1960**, 3.